Article

# Nanoparticle-Loaded Magnetophoretic Vesicles

Maren Krack, Heinrich Hohenberg, Andreas Kornowski,
Peter Lindner, Horst Weller, and Stephan Fo#rster

*J. Am. Chem. Soc.*, **2008**, 130 (23), 7315-7320 • DOI: 10.1021/ja077398k • Publication Date (Web): 17 May 2008



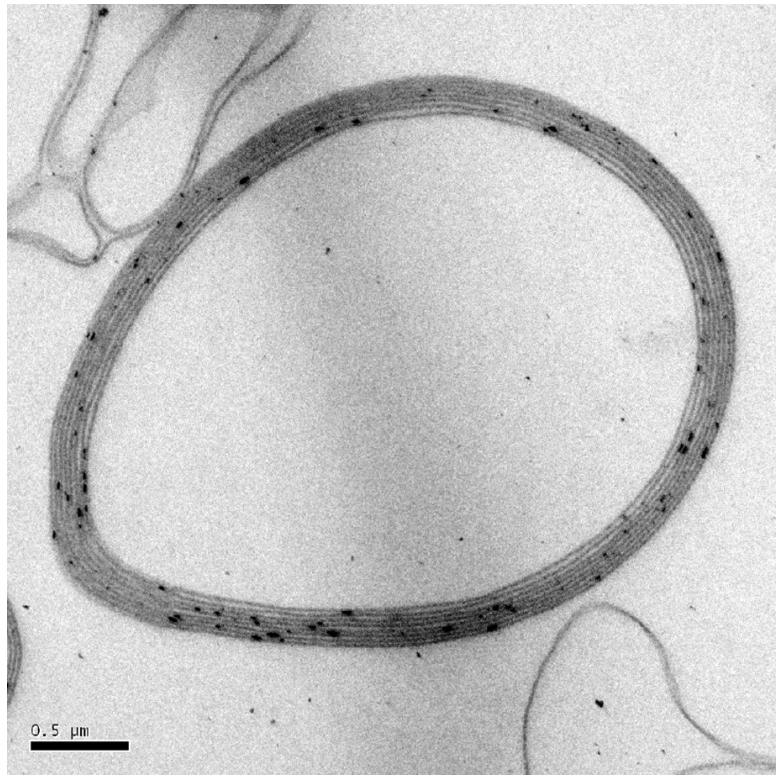

J|A|C|S
ARTICLES

Published on Web 05/17/2008

# Nanoparticle-Loaded Magnetophoretic Vesicles

Maren Krack,[†] Heinrich Hohenberg,[‡] Andreas Kornowski,[†] Peter Lindner,[§] Horst Weller,*[,†] and Stephan Förster*[,†]

*Institut für Physikalische Chemie, Universität Hamburg, Grindelallee 117, D-20146 Hamburg, Germany, Heinrich-Pette-Institut, Martinistrasse 52, D-20251 Hamburg, Germany, and Institut Laue-Langevin, 6, rue Jules Horowitz, F-38042 Grenoble Cedex 9, France*

Received September 25, 2007; E-mail: forster@chemie.unihamburg.de

Ⓦ **This paper contains enhanced objects available on the Internet at http://pubs.acs.org/jacs.**

***Abstract:*** Magnetic nanoparticles have been assembled into the bilayer membrane of block copolymer vesicles. The nanoparticles decorate the hydrophobic/hydrophilic interface, which leads to bridging of adjacent bilayers and the formation of oligo-lamellar vesicles. The nanoparticle uptake of the vesicles is sufficiently high to become magnetophoretic in external magnetic fields as shown by video microscopy.

## Introduction

Amphiphilic molecules such as surfactants, lipids, and block copolymers can self-assemble to form vesicles. Vesicles are self-supported closed bilayer assemblies of amphiphiles that enclose an aqueous interior volume.[1] Lipid vesicles or "liposomes" have received considerable attention as model systems for fluid interfaces and biomembranes[2] as well as in applications in the area of cosmetics and pharmaceutics.[3–5] In recent years, block copolymer vesicles or "polymersomes" have attracted increasing interest because of their excellent stability and the potential to control physical, chemical, and biological properties by tailoring of block lengths, block chemistry, and functionalization.[6–10]

For many biomedical applications, the controlled uptake and release of active ingredients is of particular importance. In case of block copolymer vesicles, external stimuli such as changes in pH,[11–17] temperature,[18] UV-light,[19] and concentration of oxidizing agents[20,21] can be used to trigger the release of substances in specific therapeutic windows. A further attractive external trigger for diagnostics and therapeutic treatments are external magnetic fields. Magnetic nanoparticles have been employed for magnetic resonance imaging (MRI)[22] and for magneto-thermal cancer therapy.[23] The incorporation of magnetic nanoparticles into vesicles would create a versatile diagnostic and therapeutic tool that would be biocompatible, could be magnetically moved or targeted to specific cells or organs, and could be used for controlled release stimulated by external magnetic fields. Block copolymer vesicles are particularly suited for this purpose because of their increased stability and bilayer thickness compared to lipid vesicles.

Magnetic liposomes, or "magnetoliposomes," are usually prepared by either synthesizing iron oxide nanoparticles in phosopholipid[24] or a catanionic vesicles,[25] or by coating iron oxide nanoparticles with phospholipids[26] or block copolymers such as polylysine-*b*-poly(aspartic acid).[27] These preparations result in nanoparticles having a well-defined biocompatible coating and are already in use for diagnostic and therapeutic

[†] Universität Hamburg.
[‡] Heinrich-Pette-Institut.
[§] Institut Laue-Langevin.

(1) Förster, S.; Borchert, U. Vesicles. In *Encyclopedia of Polymer Science and Technology*, 3rd ed.; Mark, H. E., Ed.; John Wiley: New York, 2005.
(2) Lipowsky, R.; Sackmann, E. *Structure and dynamics of membranes - from cells to vesicles*; Elsevier Science: Amsterdam, 1995.
(3) Ringsdorf, H.; Schlarb, B.; Venzmer, J. *Angew. Chem.* **1988**, *100*, 117.
(4) Lasic, D. D.; Papahadjopoulos, D. *Science* **1995**, *267*, 1275.
(5) Drummond, D. C.; Meyer, O.; Hong, K.; Kirpotin, D. B.; Papahadjopoulos, D. *Pharmacol. Rev.* **1999**, *51*, 691.
(6) Zhang, L. F.; Eisenberg, A. *Science* **1995**, *268*, 1728.
(7) Zhang, L. F.; Yu, K.; Eisenberg, A. *Science* **1996**, *272*, 1777.
(8) Discher, D. E.; Eisenberg, A. *Science* **2002**, *297*, 967.
(9) Lee, J. C. M.; Bermudez, H.; Discher, B. M.; Sheehan, M. A.; Won, Y. Y.; Bates, F. S.; Discher, D. E. *Biotechnol. Bioeng.* **2000**, *73*, 135.
(10) Antonietti, M.; Förster, S. *Adv. Mater.* **2003**, *15*, 1323.
(11) Ahmed, F.; Discher, D. E. *J. Controlled Release* **2004**, *96*, 37.
(12) Rodriguez-Hernandez, J.; Lecommandoux, S. *J. Am. Chem. Soc.* **2005**, *127*, 2026.
(13) Bellomo, E. G.; Wyrsta, M. D.; Pakstis, L.; Pochan, D. J.; Deming, T. J. *Nat. Mater.* **2004**, *3*, 244.
(14) Deming, T. J.; Bellomo, E. G.; Wyrsta, M.; Pakstis, L.; Pochan, D. *Polym. Mater. Sci. Eng.* **2004**, *90*, 302.
(15) Jianzhong, D.; Armes, S. P. *J. Am. Chem. Soc.* **2005**, *127*, 12800.
(16) Gohy, J.-F.; Mores, S.; Varshney, S. K.; Zhang, J.-X.; Jerome, R. *e-Polym.* **2002**, 21.
(17) Borchert, U.; Lipprandt, U.; Bilang, M.; Kimpfler, A.; Rank, A.; Peschka-Süss, R.; Schubert, R.; Lindner, P.; Förster, S. *Langmuir* **2006**, *22*, 5843.
(18) Qin, S.; Geng, Y.; Discher, D. E.; Yang, S. *Adv. Mater.* **2006**, *18*, 2905.
(19) Kros, A.; Jansen, J. A.; Holder, S. J.; Nolte, R. J. M.; Sommerdijk, N. A. J. M. *J. Adhesion Sci. Technol.* **2002**, *16*, 143–155.
(20) Napoli, A.; Valentini, M.; Tirelli, N.; Mueller, M.; Hubbell, J. A. *Nat. Mater.* **2004**, *3*, 183.
(21) Napoli, A.; Boerakker, M. J.; Tirelli, N.; Nolte, R. J. M.; Sommerdijk, N. A. J. M.; Hubbell, J. A. *Langmuir* **2004**, *20*, 3487.
(22) McCarthy, J. R.; Kelly, K. A.; Sun, E. Y.; Weissleder, R. *Nanomedicine* **2007**, *2*, 153.
(23) Jordan, A.; Wust, P.; Scholz, R. In: *Scientific and Clinical Applications of Magnetic Carriers*; Häfeli, U., Schütt, W., Teller, J., Zborowski, Z., Eds.; Plenum Press: New York, 1997.
(24) Sangregorio, C.; Wiemann, J. K.; O'Connor, C. J.; Rosenzweig, Z. *J. Appl. Phys.* **1999**, *85*, 5699.
(25) Yaacob, I. I.; Nunes, A. C.; Bose, A. *J. Colloid Interface Sci.* **1995**, *171*, 73.
(26) Gonzales, M.; Krishnan, K. M. *J. Magn. Magn. Mater.* **2005**, *293*, 265.

  

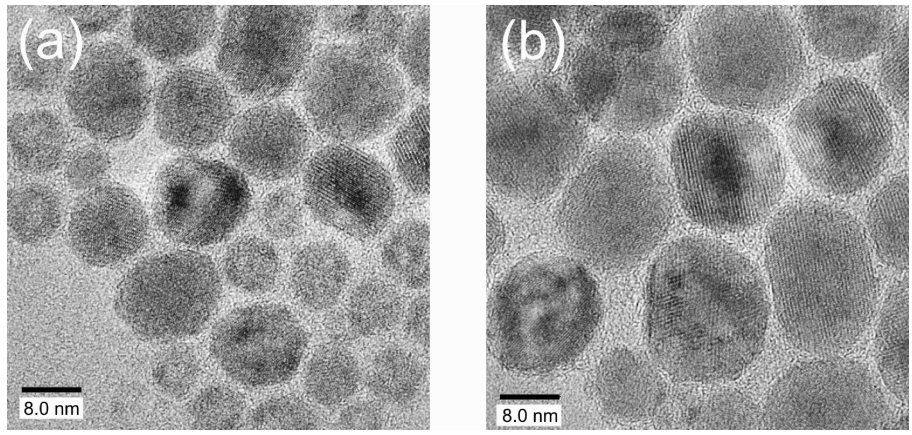


***Figure 1.*** HRTEM images of (a) 8.6 nm and (b) 14.1 nm $Fe_3O_4$ nanoparticles used for the preparation of the magnetophoretic vesicles. The single crystalline structure of the particles is clearly seen by the lattice planes.

purposes. To combine the magnetic response of nanoparticles with the targeting and release properties of vesicles, it is necessary to incorporate the nanoparticles either into the aqeous interior[28] or into the hydrophobic bilayer of intact and stable vesicles.

The incorporation of magnetic nanoparticles into liposome bilayers can be difficult, because these nanoparticles are usually much larger than the typical thickness of a lipid bilayer, that is, 3−4 nm. This problem can be overcome by using vesicle-forming amphiphilic block copolymers where the bilayer thickness can be made considerably larger. Recently, Lecommandoux indeed reported the incorporation of hydrophobic iron oxide nanoparticles into vesicle-forming polybutadiene-*b*-poly(glutamic acid) block copolymers. They observed rather aggregated but still hollow, vesicle-like structures which were deformable in external magnetic fields.[29–31]

In this article, we report for the first time the controlled preparation of well-defined magnetophoretic block copolymer vesicles with a biocompatible PEO-shell. We further demonstrate that a general effect of loading nanoparticles into vesicle bilayers is a bridging of adjacent bilayers leading to permanent connections between adjacent bilayers and the formation of oligolamellar vesicles. The obtained vesicles have biocompatible PEO-shells and are very promising as biomedical delivery vehicles with an unprecedented combination of functionalities suitable for *in vivo* magnetic localization by external magnetic fields, for magnetic resonance imaging (MRI), for magneto-thermal cancer treatment, and thermally triggered release of encapsulated hydrophilic or hydrophobic drugs.

## Materials and Methods

**Synthesis of Nanoparticles.** Magnetic $Fe_3O_4$ nanoparticles were prepared by the hot injection technique using $Fe(CO)_5$ as an iron precursor in a mixture of diphenylether and *n*-hexadecylamin as a solvent and trimethylamin-*N*-oxide as a ligand. In a typical procedure, 78 mg (1.04 mmol) of trimethylamin-*N*-oxide, 7 g (28.98 mmol) of *n*-Hexadecylamin, and 3 mL (18.86 mmol) of diphenylether were mixed at 60 °C under nitrogen and heated to 170−180 °C. After injection of 0.13 mL (0.99 mmol) of $Fe(CO)_5$, the solution was heated to 300 °C under reflux and kept at this temperature for 90 min, until the solution was cooled to 50 °C. The solution was diluted with 5 mL of chloroform, and the nanoparticles were precipitated in isopropanol. To remove excess ligands, the nanoparticles were dissolved in toluene and again precipitated in isopropanol. The size of the nanoparticles increased with increasing injection temperature, which was used to prepare $Fe_3O_4$ nanoparticles of different diameter.

The nanoparticles were characterized by high resolution transmission electron microscopy (HRTEM). Figure 1 shows that the nanoparticles represent single crystalline monodomains. The crystal structure was determined by electron diffraction (Figure S1, Supporting Information). The indicated positions of the Debye−Scherrer-rings relate to lattice plane distances of 2.94, 2.52, 2.10, 1.73, 1.63, and 1.50 Å corresponding to the (220), (311), (400), (422), (511), and (440) lattice planes of magnetite ($Fe_3O_4$). Size distribution analysis of the HRTEM-images yield a mean diameter for the $Fe_3O_4$ nanoparticles of 8.6 nm (Figure 1a) and 14.1 nm (Figure 1b), respectively.

**Synthesis of Block Copolymers.** Polyisoprene-*b*-poly(ethylene oxide) ($PI_{53}-PEO_{28}$) and poly(2-vinylpyridine-*b*-ethylene oxide) ($P2VP_{66}-PEO_{44}$) block copolymers were prepared by sequential anionic polymerization as described previously.[17,32] The subscripts indicate the degrees of polymerization. For the synthesis of PI-PEO, isoprene was condensed in into the solvent (THF) and the polymerization was initiated at −78 °C with sec-butyl lithium. After 6 h, a small amount of the obtained PI-block was quenched for polymer analytical characterization and ethylene oxide added to the reaction solution. After 2 days at 40 °C dilute acetic acid was added and the block copolymer was precipitated in methanol. For the synthesis of P2VP-PEO, 2-vinylpyridine was condensed into THF and the polymerization initiated with diphenylmethyl potassium. After 2 h, a small amount of the obtained P2VP-block was quenced for polymer analytical characterization and ethylene oxide added to the reaction solution. After 2 days at 40 °C, methanol was added and the block copolymer was precipitated in cold diethylether. All preparation procedures were carried out in an all-glass vacuum line connected to an Ar supply. The block copolymers were characterized by NMR, GPC, and MALDI-TOF-MS. The polydispersity was $M_w/M_n = 1.02$ for both block copolymers.

**Sample Preparation.** The nanoparticles were loaded into the hydrophobic interior of the vesicle bilayer by using film rehydration or a reverse phase transfer method. For film rehydration, 0.5 mL of a solution of the block copolymer in chloroform (10 mg/mL)

(27) Euliss, L. E.; Grancharov, S. G.; O'Brien, S.; Deming, T. J.; Stucky, G. D.; Murray, C. B.; Held, G. A. *Nano Lett.* **2003**, *3*, 1489.
(28) Martina, M.-S.; Fortin, J.-P.; Menager, C.; Clement, O.; Barratt, G.; Grabielle-Madelmont, C.; Gazeau, F.; Cabuil, V.; Lesieur, S. *J. Am. Chem. Soc.* **2005**, *127*, 10676.
(29) Lecommandoux, S.; Sandre, O.; Checot, F.; Rodriguez-Hernandez, J.; Perzynski, R *Adv. Mater.* **2005**, *17*, 712.
(30) Lecommandoux, S.; Sandre, O.; Checot, F.; Perzynski, R. *Prog. Solid State Chem.* **2006**, *34*, 171.
(31) Lecommandoux, S.; Sandre, O.; Checot, F.; Rodriguez-Hernandez, J.; Perzynski, R. *J. Magn. Magn. Mater.* **2006**, *300*, 71.
(32) Förster, S.; Krämer, E. *Macromolecules* **1999**, *32*, 2783.

was mixed with 0.5 mL of a solution of $Fe_3O_4$ nanoparticles in chloroform (2 mg/mL). Chloroform was evaporated by gentle shaking in a 50 mL reaction flask to obtain a thin film inside the flask. The addition of 5 mL of deionized water (Millipore) leads to swelling and the formation of vesicles within 2−3 days, yielding a turbid, brownish solution. This procedure yields a mass ratio of nanoparticle to polymer of $r = 0.2$. The mass ratio can be varied by mixing different volumes of the respective chloroform solutions. For the reverse phase transfer method, 0.5 mL of a solution of the block copolymer in chloroform (10 mg/mL) was mixed with 0.5 mL of a solution of $Fe_3O_4$ nanoparticles in chloroform (2 mg/mL) and covered with a 5 mL deionized water layer. During evaporation of the chloroform over a period of 2−3 days, the block copolymer with the nanoparticles is continuously transferred into the aqueous phase to form vesicles until the chloroform phase has completely evaporated under gentle stirring. Both methods routinely yield slightly turbid, brownish aqueous solutions of vesicles of several micrometers diameter for PI-PEO and P2VP-PEO block copolymers. The vesicles are polydisperse having diameters between 0.5 and 20 $\mu$m. The film rehydration methods has a tendency to yield a larger fraction of large vesicles, which is why it was used for the magnetophoretic studies. The vesicles can be extruded through membrane filters to diameters of 0.5 $\mu$m with a more homogeneous size distributions.

**Characterization Methods.** HRTEM was performed on a Philips CM-300 UT microscope operated at 300 kV. Samples were prepared by deposition of toluene or chloroform solutions onto carbon-coated copper grids. Cryo-TEM was performed on a Philips CM 120 operated at 80 kV. Samples were prepared by high-pressure freezing and freeze-substitution[33] followed by low-temperature embedding in Spurr low viscosity resin and by ultrathin sectioning of the polymerized resin block. SANS-measurements were carried out at the 5.0 and 1.1 m detector position at the small-angle neutron scattering instrument D11 at ILL, Grenoble. The neutron wavelength was $\lambda = 0.6$ with $\Delta\lambda/\lambda = 9\%$ (fwhm). Details of the instrumentation and data reduction can be found elsewhere.[34] The polymer concentration was 5 g/L in $D_2O$. Video microscope was performed on an inverted microscope Axiovert S100 from Zeiss equipped with a CCD camera (Zeiss AxioCam HRc) and a video camera (JVC, TKC1381).

**Magnetophoretic Measurements.** For the magnetophoretic measurements, a drop of an aqueous vesicle solution was placed on a glass slide, covered with a cover slide to prevent evaporation and convection, and mounted on the stage of an inverted optical microscope. A small 5 mm diameter by 2 mm thick Nd-magnet mounted on a pencil was placed directly above the cover slide in 3 mm distance to the center of the cover slide which is located in the optical axis of the microscope where the magnetophoretic motion is imaged. To demonstrate that the motion of the vesicles was not due to diffusion or convection, the magnet was moved to different positions with respect to the center of the cover slide to induce motion of the vesicles in the respective direction. A Ⓦ video of vesicles moving toward the magnet at different positions is provided. For theoretical calculations, the magnetization curves of the nanoparticles and the magnetic field gradient of the Nd magnet are provided in the Supporting Information. At 3 mm distance, the magnetic field gradient is $dB/dx = 50$ mT/mm, the magnetic flux density is $B = 120$ mT (see Figure S2, Supporting Information), and the magnetization of the nanoparticles is $M = 27$ emu/g (see Figure S3, Supporting Information).

## Results and Discussion

**Small-Angle Neutron Scattering.** The unloaded block copolymer vesicles were characterized by small-angle neutron scattering (SANS) to determine the bilayer thickness. For a bilayer the measured intensity $I(q)$ as a function of the scattering vector $q$ is given by

$$I(q) = I_0 \frac{4J_1^2(qR_D)}{q^2R_D^2}\left\langle \frac{\sin^2(qd/2)}{q^2d^2/4} \right\rangle \quad (1)$$

where $I_0$ is proportional to the primary beam intensity, $J_1(z)$ is the Bessel function, and $R_D$ and $d$ are the lateral extension and the thickness of the bilayer, respectively. The experimental data were fitted to eq 1 to obtain a bilayer thickness of $d = 11.7$ nm for the PI-PEO vesicles and $d = 12.3$ nm for the P2VP-PEO vesicles. The data together with the fitted scattering curves are shown in Figure 2.

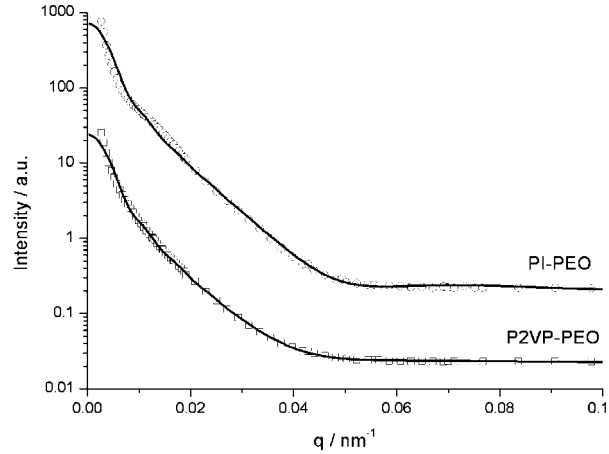


***Figure 2.*** Measured and fitted SANS-curves of unloaded PI-PEO (○) and P2VP-PEO (□) vesicles. The thickness of the PI-PEO bilayer is 11.7 nm, and it is 12.3 nm for the P2VP-PEO bilayer.

**Nanoparticle-Induced Bilayer Pairing.** We have found that an important parameter for the preparation of stable nanoparticle-loaded vesicles is the mass ratio $r = m_n/m_p$ of nanoparticles, $m_n$, to polymer, $m_p$. If this ratio is larger than $r^* \approx 0.2-0.3$, then the formation of polymer/nanoparticle agglomerates is observed for both block copolymers and both vesicle preparation methods. A mechanism for this agglomerate formation is discussed below. Below the ratio $r^*$, the preparation of stable vesicles is routinely achieved.

To investigate details of the vesicle structure and the location of nanoparticles within the vesicle bilayer, we performed cryo-transmission electron microscopy using a specially adapted sample preparation procedure for contrast enhancement of the PI-PEO bilayers.[35] Cryo-electron micrographs were prepared from ultrathin sections of solidified embedded solutions, where the polyisoprene-block was stained with $OsO_4$ and the PEO-block stained with uranyl acetate. The four cryo-TEM images in Figure 3 are taken from a large series of images and exemplarily show typical morphologies observed in solutions of PI-PEO vesicles. Because the cryo-TEM imaging method is rather elaborate, we focused on vesicles with a loading ratio that is as high a possible, that is, $r = 0.2$ mg nanoparticles/mg polymer, but not yet in a range where vesicle aggregation is observed. All vesicle solutions for the cryo-TEM studies were prepared by the reverse phase transfer method and loaded with 14.1 nm $Fe_3O_4$ nanoparticles.

(33) Hohenberg, H.; Mannweiler, K; Müller, M *J. Microsc.* **1994**, *175*, 34–43.
(34) Lindner, P., Zemp, T. *Neutrons, X-rays and Light: Scattering Methods Applied to Soft Condensed Matter*; Elsevier: Amsterdam, 2002.
(35) Kirschning, E.; Rutter, G.; Hohenberg, H. *J. Neurosci. Res.* **1998**, *53*, 465–474.

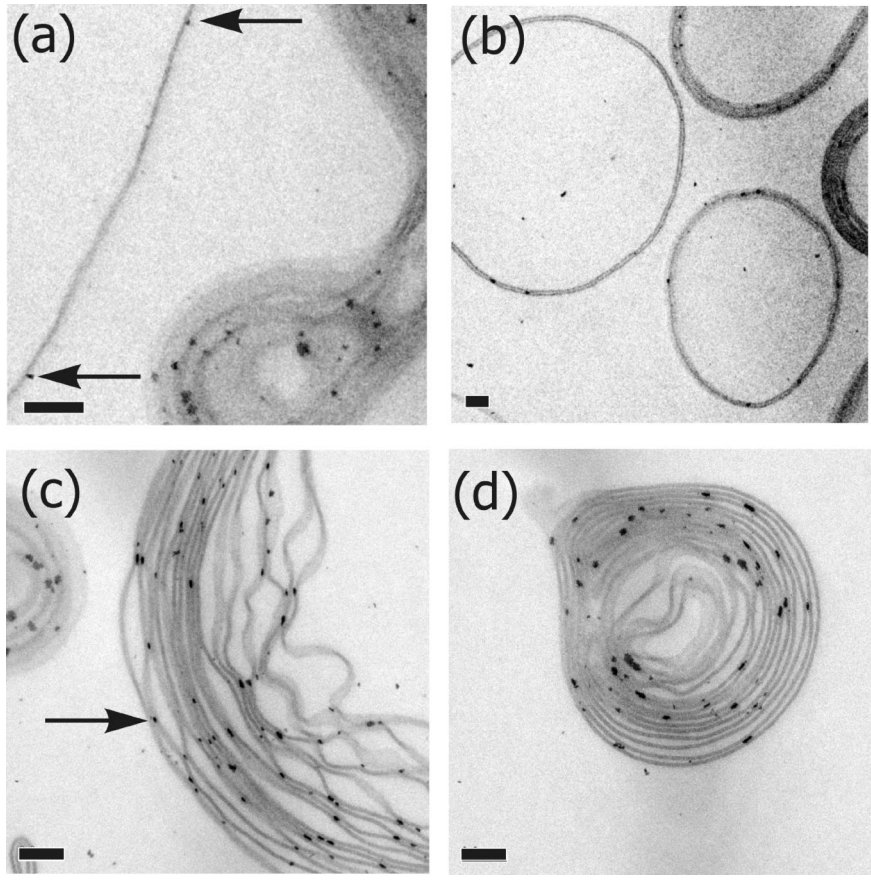


***Figure 3.*** Cryo-TEM images of 14.1 nm $Fe_3O_4$ nanoparticles loaded into PI-PEO vesicle bilayers. (a) Nanoparticles (arrows) incorporated into a single bilayer, (b) oligo- and multi lamellar vesicles, (c) stable nanoparticle connections (arrow) between adjacent bilayers, and (d) onion-like vesicles. The scale bar is 200 nm. The figures shows typical morphologies present in a vesicle solution at a loading ratio of $r = 0.2$.

Figure 3a shows a TEM-image of a single bilayer. The total thickness of the PI-PEO bilayer as determined from the cryo-TEM images is 12 nm which is in good agreement with a value of 11.7 nm determined by SANS. A weight ratio of $r = 0.2$ corresponds to a volume ratio of $r_V = 0.04$ (4%), which is in agreement with the loading ratio apparent from the cryo-TEM images, that is, in Figure 3d. We observe that the hydrophobic nanoparticles are not located in the center of the bilayer but rather at the periphery decorating the hydrophobic/hydrophilic PI/PEO-interface (arrows). This is a general phenomenon for particles with a hydrophobic/lipophilic balance (HLB) between the hydrophobic phase (PI) and the hydrophilic phase (PEO/water). Such particles will preferentially segregate to the hydrophobic/hydrophilic interface with a penetration depth into the hydrophobic domain depending on its HLB value.[36] Because the entropy of mixing between particles and polymers is generally very low, complete miscibility and thus complete localization of the nanoparticles at the center of the PI domain would be expected only in case of perfect compatibilization of the nanoparticle/PI-interface.

The nanoparticles decorating the interface lead to a tendency to bridge to an adjacent bilayer. This bridging leads to bilayer pairing, which is schematically shown in Figure 4. Bridged bilayers are observed in most cryo-electron micrographs such as in panels b−d of Figures 3. These connections are stable because the interfacial energy of a nanoparticle is lowered by

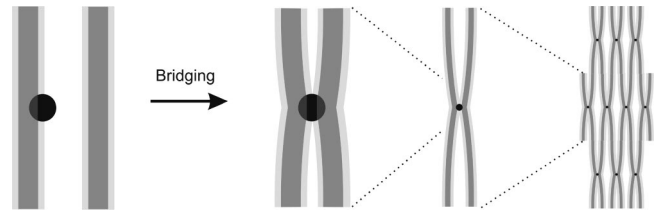


***Figure 4.*** Scheme of nanoparticle-induced bilayer pairing and bridging. The nanoparticles are located in the hydrophobic/hydrophilic interface. The right-hand structure compares well to the bridged structures observed in Figure 3c.

contact with two instead of one interface. A contact with three or more interfaces, which would further lower the interfacial energy of a nanoparticle, is topologically impossible for bilayers.

The formation of bridges leads to an increased tendency to form oligo- and multilamellar vesicles such as in Figure 3b and c, or even onion-type vesicles such as in Figure 3d. From our cryo-TEM investigations we observe a trend to form oligo-lamellar vesicles with an even number of bilayers, that is, bilayer pairs, with a number of 2, 4, 6, and 8 bilayers per vesicle (e.g., Figure 3b). Unilamellar vesicles are rarely observed, as are vesicles with a significantly larger number of bilayers. Without nanoparticles the block copolymers form exclusively unilamellar vesicles for the same sample preparation conditions. Bilayer bridging may also explain the formation of aggregated vesicular structures for loading ratios $r > r^*$ and explain observations of nanoparticle-induced vesicular aggregation reported in literature.[29–31]

(36) Antonietti, M. *Angew. Chem.* **1988**, *100*, 1813.

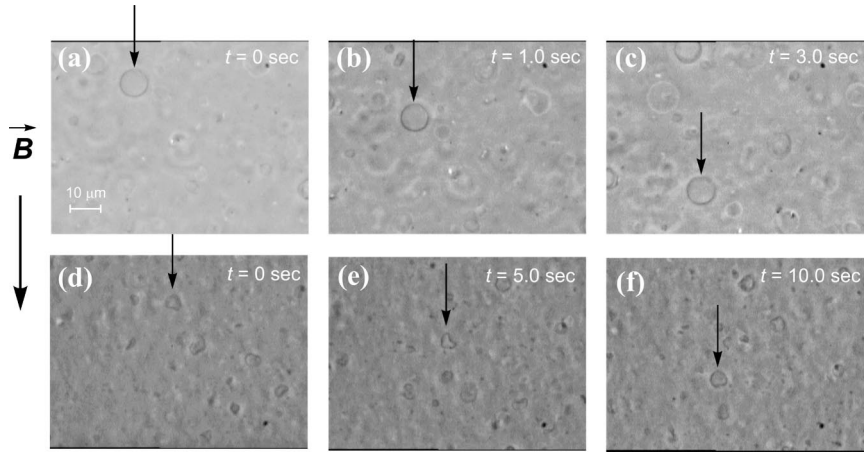


***Figure 5.*** Series of video microscopy snapshots showing the magnetophoretic mobility of PI-PEO (a−c) and P2VP-PEO (d−f) vesicles loaded with 8.6 nm $Fe_3O_4$-nanoparticles. The positions of single moving vesicles are marked by an arrow. The vesicles have mobilities of 3 $\mu$m/s (P2VP-PEO) and 12 $\mu$m/s (PI-PEO) when using a small 5 mm diameter Nd-magnet at a distance of 3 mm from the sample.

Although limiting the nanoparticle/polymer mass ratio $r$, bilayer bridging nevertheless leads to a loading capacity for hydrophobic nanoparticles that is sufficiently high to yield magnetophoretic vesicles. As the aqueous interior of the vesicles is large enough for the encapsulation of hydrophilic active agents, these vesicles are well suited for applications where the magnetic response (e.g., mobility, contrast, magneto-thermal response) is to be coupled to a triggered release.

**Magnetophoretic Mobility.** The forces that act on a magnetic vesicle at steady state in an external magnetic field are given by the force due to the magnetic field gradient, $F_B$, and the viscous drag, $F_v$, acting against it. The two forces are given by

$$F_B = m\frac{dB}{dx} \tag{2}$$

$$F_v = 6\pi\eta R v \tag{3}$$

where $m$ is the magnetic moment of the vesicle, $dB/dx$ is the gradient of the magnetic field, $\eta$ is the viscosity of the solvent, $R$ is the hydrodynamic radius, and $v$ is the velocity of the particle. The magnetic moment $m$ is directly related to the magnetization: $M = m/V$, where $V = 4\pi R^3/3$ is the vesicle volume. At steady state, the force balance leads to a magnetophoretic mobility of

$$v = \frac{2MR^2}{9\eta}\frac{dB}{dx} \tag{4}$$

The magnetophoretic mobility should increase with increasing radius, because the magnetic force scales in proportion to $R^3$ for solid particles or $R^2$ for unilamellar vesicles, whereas the viscous force is linearly proportional to $R$.

For the magnetophoretic measurements a drop of an aqueous vesicle solution was placed on a glass slide, covered with a cover slide to prevent evaporation and convection, and mounted on the stage of the optical microscope. We used a small 5 mm diameter 2 mm thick Nd magnet in close proximity to the sample that was placed under the optical microscope. The magnetic flux density was measured with a Hall-probe as a function of distance (see Figure S3 in Supporting Information). At contact the flux density is 425 mT decaying to less than 20 mT at distances larger than 10 mm. At a sample to magnet distance of 3 mm as used in the experiment, the magnetic field gradient as depicted in Figure S1 (see Supporting Information) is $dB/dx$ = 50 mT/mm.

Using video microscopy, we observe that despite the small volume fraction of nanoparticles with respect to the total volume of micrometer-sized vesicles, the vesicles migrate in an external magnetic field. Figure 5 shows a series of snapshots taken during migration of PI-PEO vesicles (Figure 5a−c) and P2VP-PEO vesicles (Figure 5d−f) prepared by film rehydration loaded with 8.6 nm $Fe_3O_4$-nanoparticles at a ratio of $r = 0.1$ mg nanoparticles/mg polymer. The vesicles have mobilities in the range of 12 $\mu$m/s for the PI-PEO vesicle (Figure 5a−c) and 3 $\mu$m/s for the P2VP-PEO vesicle (Figure 5d−f) when using a small 5 mm diameter Nd-magnet with a distance of 3 mm from the sample. This mobility is remarkable in view of the very low volume fraction of magnetic nanoparticles.

From eq 4 we can make an estimate of the theoretically expected magnetophoretic mobility of the vesicles. Considering PI-PEO vesicles with a radius of $R = 5$ $\mu$m as in the first series of video snapshots (Figure 5a−c) with a bilayer thickness of $d$ = 12 nm (see Figure 2), the volume fraction of the bilayer is equal to $\varphi_v = 1 - (R - d)^3/R^3$. With the volume fraction $\varphi_v$ we can calculate the magnetization $M$ of the vesicles as

$$M = \varphi_v r \rho l \chi_{Fe_3O_4} \tag{5}$$

with a mass ratio of $r = 0.1$ as in Figure 5, $\rho = 1$ g/mL as the average volume density of the water-filled vesicle, $l$ the lamellarity of the vesicles which for the present calculation is assumed to be $l = 2$, and a mass susceptibility of $\chi_{Fe_3}O_4 = 27$ emu/g of the magnetite nanoparticles obtaining a value of $M$ = 39 A/m. Inserting this in eq 4 with a magnetic field gradient of $dB/dx = 50$ T/m and a viscosity of water of $\eta = 1.0$ mPas, we calculate a magnetophoretic mobility of $v = 11$ $\mu$m/s, which is in good agreement with the experimentally determined value of 12 $\mu$m/s. For the smaller P2VP-PEO vesicle (Figure 5d−e, $R = 3$ $\mu$m), we calculate a smaller magnetophoretic mobility of $v = 6$ $\mu$m/s, which is, however, larger than the experimentally determined value of 3 $\mu$m/s, possibly due to the irregular shape of the vesicle leading to internal rotational modes of motion. These calculations show that the measured magnetophoretic mobilities are in range that is theoretically expected.

## Conclusions

In conclusion, we have shown that hydrophobic magnetic nanoparticles can well be incorporated into the bilayers of block copolymer vesicles. The incorporation of nanoparticles into the

bilayer causes bridging of adjacent bilayers leading to an increased tendency to form oligo- and multilamellar vesicles. The increased lamellarity of the vesicles leads to a higher loading of magnetic nanoparticles which enhances magnetophoretic mobility in external magnetic fields. The vesicles have biocompatible PEO-shells and are very promising as delivery vehicles with an unusual combination of functionalities suitable for *in vivo* magnetic localization by external magnetic fields, for providing contrast for magnetic resonance imaging (MRI), for magnetothermal treatment of cancer by inductive heating of the nanoparticles coupled to a thermally triggered release of encapsulated hydrophilic or hydrophobic drugs.

**Acknowledgment.** We thank U. Tromsdorf and U. König for the magnetization measurements.

**Supporting Information Available:** Figures S1−S3 and further information. This material is available free of charge via the Internet at http://pubs.acs.org.

JA077398K